nature chemistry

ARTICLES

PUBLISHED ONLINE: 22 NOVEMBER 2009 | DOI: 10.1038/NCHEM.446

# Template synthesis of precisely monodisperse silica nanoparticles within self-assembled organometallic spheres

Kosuke Suzuki[1], Sota Sato[1] and Makoto Fujita[1,2]*

**One of the key challenges in materials science is to control the size and shape of inorganic nanoparticles with a high degree of precision, as these parameters have a significant influence on the nanoparticles' properties and potential applications. Here, we describe the preparation of highly monodisperse silica nanoparticles smaller than 5 nm in diameter by using self-assembled, hollow, spherical compounds as 'endo-templates'. These coordination complexes with pendant sugar groups lining their interiors—assembled from 12 metal ions and 24 bis-pyridyl ligands containing glucose substituents—acted as structurally well-defined templates for the sol–gel condensation of alkoxysilanes. The polydispersities of the silica nanoparticles made with this method approached unity, with $M_w/M_n < 1.01$. The component ligands are modified easily, which enables an accurate expansion of the coordination complex and the subsequent control of the monodisperse silica nanoparticles that span molecular weights of 5,000 to 31,000 Da (corresponding to 2–4 nm in diameter). This method could be applicable to the preparation of other inorganic nanoparticles.**

The precise control of the shape and the size of inorganic nanoparticles is of great importance in materials science because the ability to control the bulk properties at the molecular level could generate new applications[1,2]. The most-efficient methods used to prepare controlled nanoparticles exploit hollow structures as endo-templates to restrict their size and shape[3–7]. Polymer capsules such as micelles are commonly used[8–11], but are imprecise templates as they are structurally ill-defined. Biological structures[12–16], such as ferritin[17–19], are well-defined and can be used to template particles on a nanometre scale, but difficulties with template modification limit their utility.

Here, we report the preparation of highly monodisperse silica nanoparticles by using self-assembled organometallic spheres as endo-templates. The spheres were assembled from 12 metals (M) and 24 organic ligands (L) and possessed a rigid and well-defined framework that could be expanded precisely to a diameter of 6.3 nm. When the sphere interiors were lined with sugar residues, the spheres acted as a precise endo-template for the sol–gel condensation of tetramethoxysilane (TMOS). Remarkably, the weight-averaged ($M_w$) and number-averaged ($M_n$) molecular weights indicate a polydispersity that approaches unity ($M_w/M_n$ <1.01). The component ligands are modified easily by organic synthesis, which enables an accurate expansion of the molecule and subsequent control of monodisperse silica nanoparticles that span molecular weights of 5,000 to 31,000 Da, corresponding to 2–4 nm in diameter. These results lead to a new method for the discrete synthesis of highly monodisperse inorganic nanoparticles (such as metal clusters, metal oxides and coordination networks) at a scale of less than 10 nm.

## Results and discussion

The 5 nm $M_{12}L_{24}$ organometallic spheres[20] self-assembled quantitatively as a result of mixing $Pd(NO_3)_2$ and bis(4-pyridyl)-substituted bent ligands **1** (Fig. 1). Modification of the periphery[20,21] and interior[22–24] of the giant spheres was achieved by simply attaching the desired group at the apex or nadir of ligand **1** before self-assembly. Ligand **1a** was designed so that the 24 pendant glucose units would line the sphere interior (Fig. 1)[25]. These glucose units acted as an endo-template for the sol–gel condensation of alkoxysilanes and the formation of silica nanoparticles based on the reversible condensation reaction between silanols and sugars. Treatment of ligand **1a** with $Pd(NO_3)_2$ (0.5 equiv.) in dimethylsulfoxide (DMSO)-$d_6$ for one hour at 50 °C resulted in the quantitative formation of sugar-lined complex **2a**. $^1$H NMR spectroscopy and cold-spray ionization mass spectrometry (CSI-MS)[26] of complex **2a** confirmed an $M_{12}L_{24}$ assembly with a molecular mass of 14,826 Da (see Supplementary Information).

After confirming the self-assembly of sphere **2a**, the condensation of TMOS was examined. A DMSO-$d_6$ solution of **2a** was diluted with $CDCl_3$ (DMSO-$d_6$:$CDCl_3$ = 1:9, Fig. 2a) and 170 equivalents of TMOS and 100 equivalents of $H_2O$ were added. The mixture was stirred at room temperature for four days and monitored by $^1$H NMR. The Si$OCH_3$ signals decreased and the signals from methanol increased, which was attributed to the hydrolysis of TMOS, and the signals of the framework of **2a** broadened (Fig. 2b–d). The solution remained clear and the silica gel did not precipitate, which suggested that the condensation occurred within sphere **2a**. After sphere **2a** had been isolated and washed with excess methanol to remove residual silica, X-ray fluorescence (XRF) analysis of the resultant powder showed the Si:Pd ratio to be 167:12 (which corresponds to Si:**2a** = 167:1) and indicated that all the TMOS reacted within the sphere. When the sol–gel condensation of TMOS was examined in the presence of **2b**, which lacks interior glucose units, the condensation proceeded in the bulk solvent. After four days, the $^1$H NMR signals of **2b** did not change and silica gel precipitated from the reaction mixture.

The condensation reaction of TMOS only occurred within the cavity of sphere **2a** and no intermolecular cross-linking between spheres

[1]Department of Applied Chemistry, School of Engineering, The University of Tokyo, Hongo, Bunkyo-ku, Tokyo, 113-8656, Japan, [2]Core Research for Evolutional Science and Technology (CREST), Japan Science and Technology Agency (JST), Hongo, Bunkyo-ku, Tokyo, 113-8656, Japan.
*e-mail: mfujita@appchem.t.u-tokyo.ac.jp

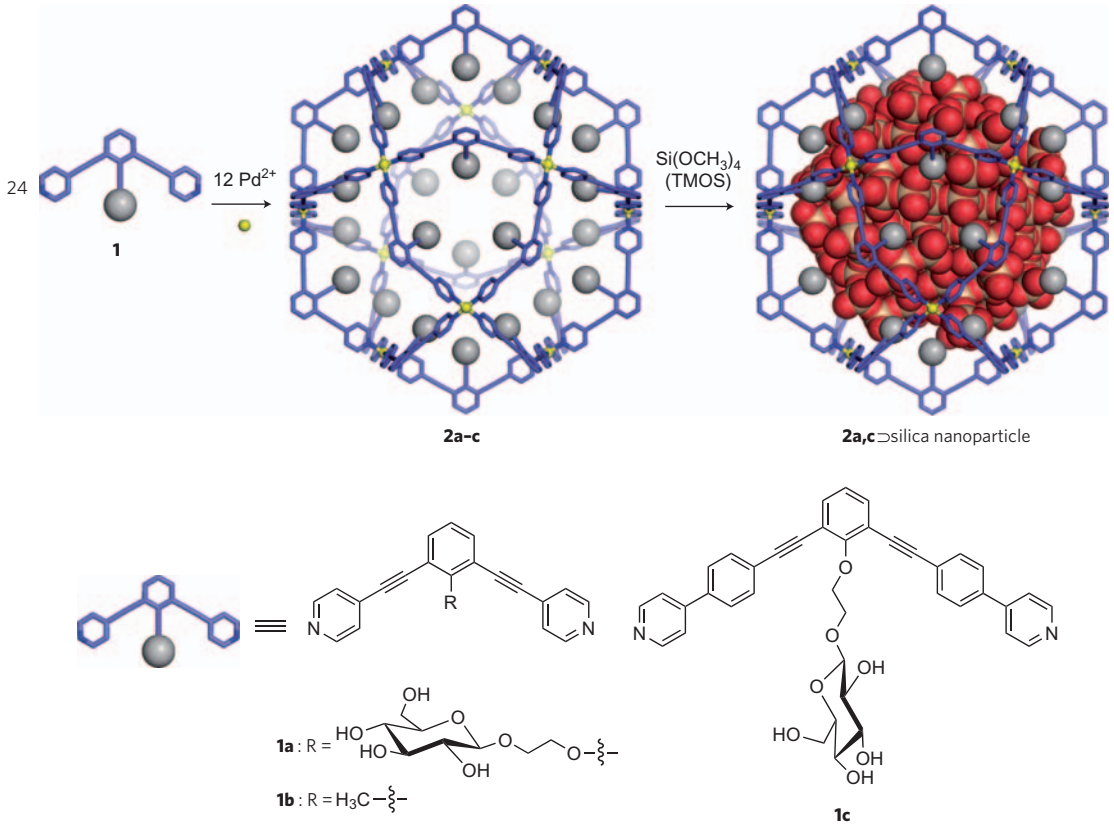


**Figure 1 | Synthesis of silica nanoparticles within spheres 2.** Spheres **2a**,**b** (4.6 nm) and **2c** (6.3 nm) quantitatively self-assembled from ligands **1a**–**c** and Pd(II) ions in DMSO. The sol–gel condensation of TMOS was carried out in the presence of **2a** or **2c** (DMSO–$CHCl_3$–$H_2O$, room temperature, four days) to form monodisperse silica nanoparticles within the spherical shells of **2a**,**c**.

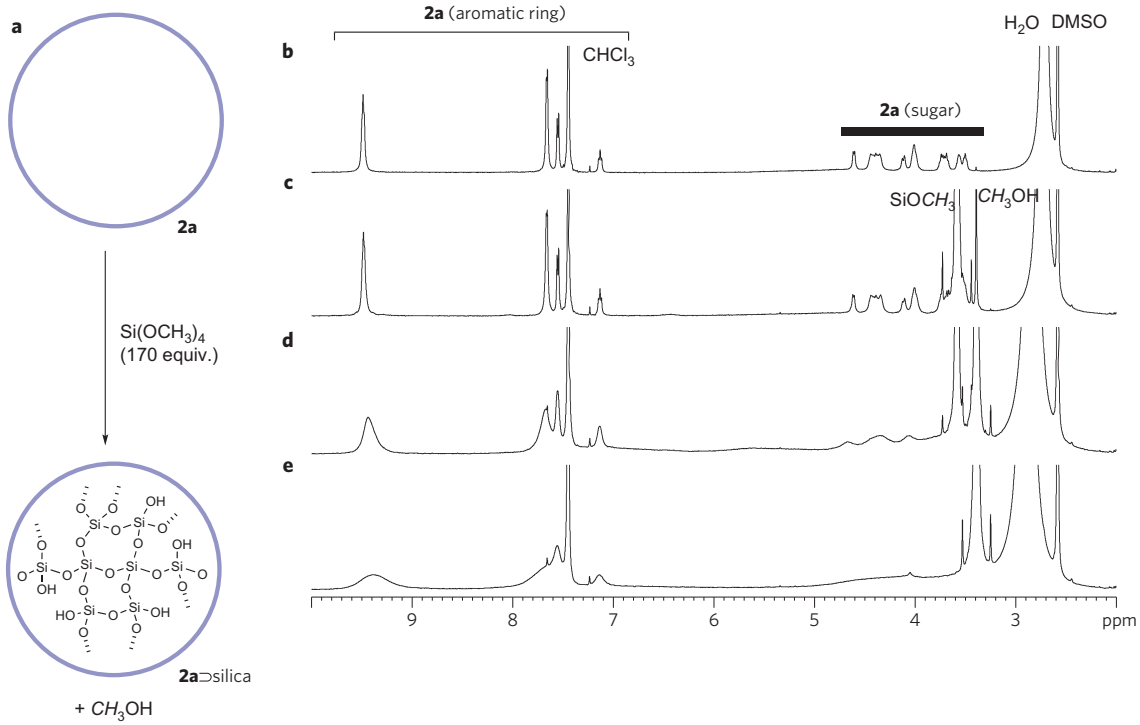


**Figure 2 | $^1$H NMR spectra (500 MHz, 300 K, DMSO-$d_6$:$CDCl_3$ = 1:9) of sphere 2a and 2a⊃silica. a**, Schematic representation of the formation of silica nanoparticles within sphere **2a** by the condensation of TMOS. **b**, Spectrum of sphere **2a** before the addition of TMOS. **c**–**e**, Spectra after condensation of TMOS (170 equiv.) in the presence of **2a** at room temperature in DMSO-$d_6$/$CDCl_3$ (**c**, 30 minutes; **d**, ten hours; **e**, four days). As the hydrolysis of TMOS proceeded, the signal of methanol increased. At the same time, the shell framework of **2a** broadened significantly, which shows the formation and the growth of a silica nanoparticle within **2a**.

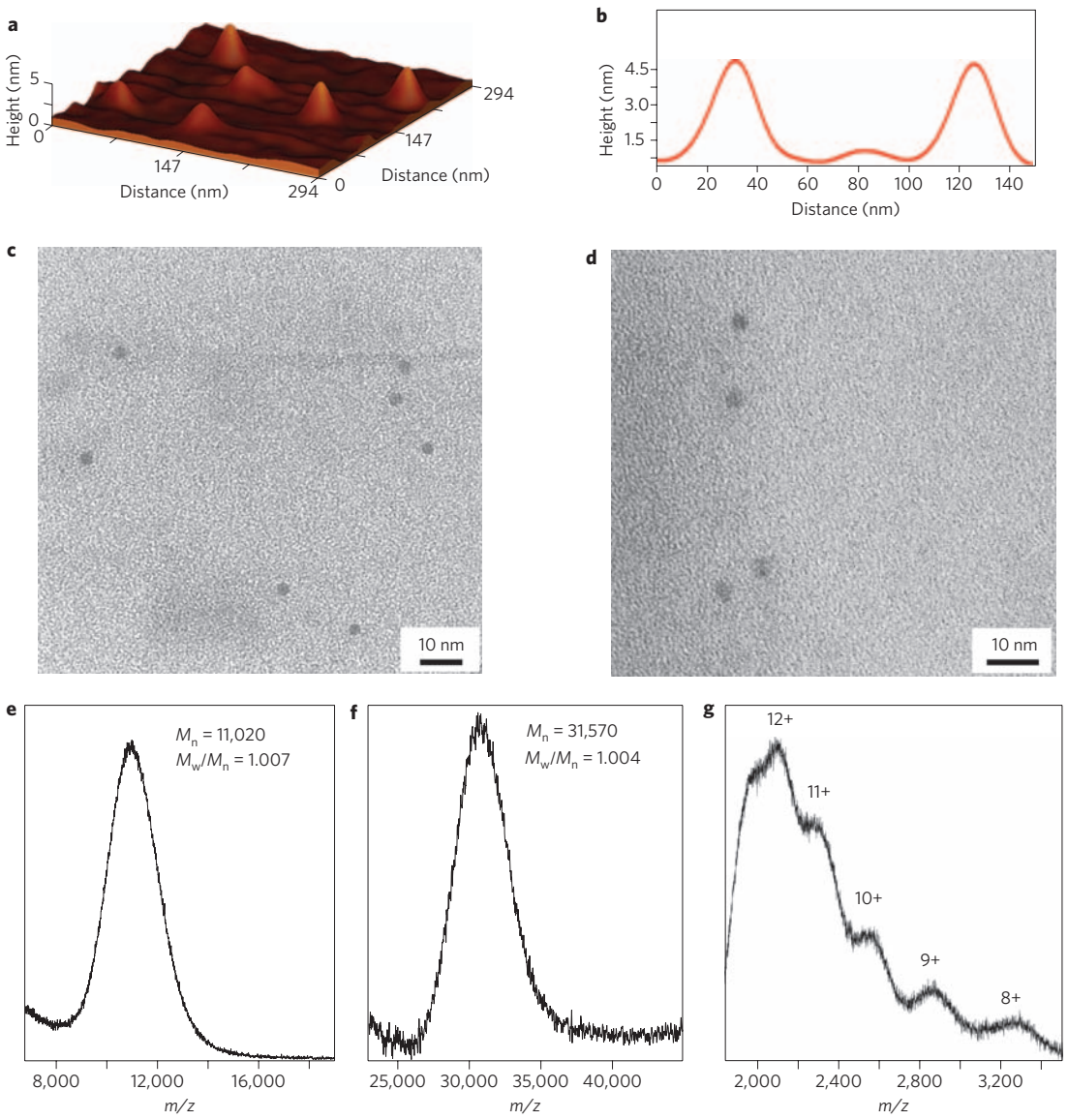


**Figure 3 | Structural analyses of silica nanoparticles within spherical templates. a**, AFM image of **2a**⊃silica on mica. **b**, Height profile of AFM image for **2a**⊃silica. Separated particles with heights of 4.6±0.2 nm were observed. **c**, TEM image of silica nanoparticles formed within **2a**. The average diameter of silica nanoparticles was 2.9 nm, which is consistent with the modelled silica nanoparticles with 170 $SiO_2$ units. **d**, TEM image of silica nanoparticles formed within **2c**. The average diameter of silica nanoparticles was 4.0 nm. **e**, LDI-MS spectrum of silica nanoparticles ($M_n$ = 11,020; $M_w/M_n$ = 1.007) within **2a** after reaction with 170 equivalents of TMOS. **f**, LDI-MS spectrum of silica nanoparticles ($M_n$ = 31,570; $M_w/M_n$ = 1.004) within **2c** after reaction with 500 equivalents of TMOS. **g**, CSI-MS spectrum of **2a**⊃silica after reaction with 170 equivalents of TMOS ($n+ = [\mathbf{2a} + \text{silica-}(NO_3)_n]^{n+}$).

occurred. The diffusion coefficient of **2a** ($1.5 \times 10^{-10}$ $m^2$ $s^{-1}$) was determined by diffusion-ordered NMR spectroscopy experiments and remained constant before and after the condensation reaction. Atomic force microscopy (AFM) clearly showed well-separated particles with a uniform height (4.6±0.2 nm), consistent with the diameter of framework of **2a**, 4.6 nm (Fig. 3a,b).

The rigid shell framework of **2a** favours crystallization and single crystals of **2a**⊃silica, after the reaction with 170 equivalents of TMOS, were obtained by slow vapour diffusion of chloroform into a solution of **2a**⊃silica (counter ion, $BF_4^-$). Although single crystals of **2a**⊃silica provided weak diffractions because of the large unit cell and severely disordered solvent molecules, synchrotron X-ray analysis revealed that the robust framework of sphere **2a**, with a diameter of 4.6nm, remained intact even after formation of the silica nanoparticle (Fig. 4a). The sugar-coated interior of **2a** and the incarcerated silica nanoparticle are, unfortunately, rather amorphous and severely disordered.

The silica nanoparticle, which consisted of 170 $SiO_2$ units and had a diameter of about 2.8 nm, was modelled within the structure of the shell framework of **2a** as determined by an X-ray diffraction study. This combined structure of **2a**⊃silica clearly shows that the cavity of **2a** comfortably accommodates the silica nanoparticle of 2.8 nm (Fig. 4b). Transmission electron microscopy (TEM) images confirmed our predictions and revealed the average diameter of silica nanoparticles to be 2.9 nm (Fig. 3c). No image was obtained for the empty sphere **2a**. Energy-dispersive X-ray analysis of the **2a**⊃silica nanoparticles confirmed the presence of both silica and palladium atoms (see Supplementary Information), and showed that the observed TEM image (Fig. 3c) is derived from the silica nanoparticles within the shell.

The molecular mass of the silica nanoparticle formed in **2a** was measured directly by laser desorption ionization mass spectrometry (LDI-MS). Under LDI conditions, the $M_{12}L_{24}$ framework of **2a** decomposes and is not observed. Thus, when **2a**⊃silica was

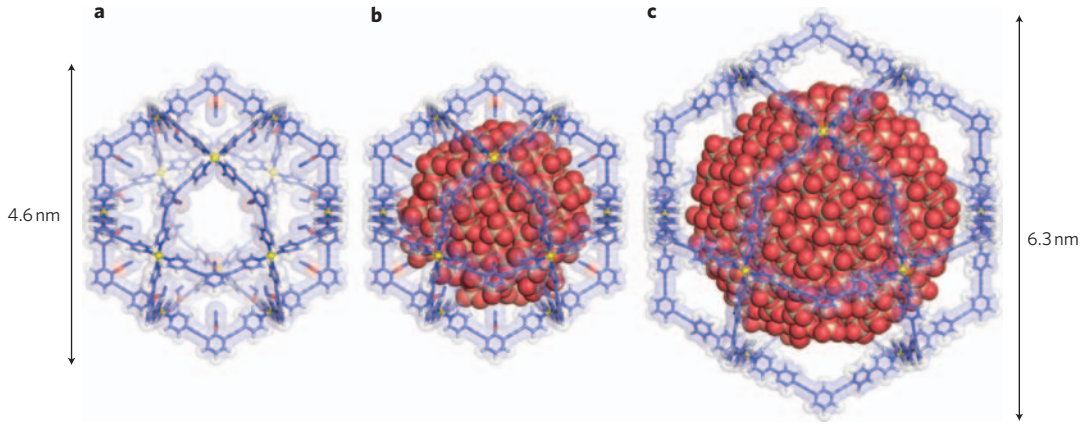


**Figure 4 | Molecular structures of spheres 2a,c that contain silica nanoparticles. a**, The structure of the shell framework of **2a**, which accommodates a silica nanoparticle within the cavity, was determined by an X-ray diffraction study. Structural analysis showed that the shell of **2a** (4.6 nm) was completely maintained even after formation of the nanoparticle. The glucose residues and silica nanoparticle within **2a** could not be revealed because of severe disordering. **b**, A silica nanoparticle (2.8 nm), consisting of 170 $SiO_2$ units, was modelled and combined with the determined structure of the shell of **2a**. The silica nanoparticle was represented by space-filling models. **c**, Molecular modelling of silica nanoparticles (4.0 nm) of 500 $SiO_2$ units combined with the shell framework of **2c**.

subjected to the LDI-MS analysis, only silica$^+$ was observed at $m/z = \sim$11,000 (Fig. 3e). The calculated $M_w$ and $M_n$ (11,100 and 11,020, respectively) indicated a polydispersity ($M_w/M_n$) near unity (1.007). Organometallic sphere **2a** was a successful template for almost perfectly monodisperse silica nanoparticles. Within the protective sphere, the silica nanoparticle is very stable, and the molecular mass of the silica nanoparticle remained unchanged even after six months. Under the gentle conditions of CSI-MS, the $M_{12}L_{24}$ framework is maintained and observable (Fig. 3g). The CSI-MS spectrum of **2a**⊃silica shows a series of broad peaks assigned to $[\mathbf{2a} + \text{silica}–(NO_3)_n]^{n+}$ ($n = 8$–12). From these peaks, the molecular mass of the silica nanoparticle formed in **2a** was calculated to be 11,200, in good agreement with the LDI-MS results.

The size of the silica nanoparticle is defined by the spherical shell, and larger monodisperse silica nanoparticles can be prepared by expanding the diameter of the sphere. Ligand **1c**, with an additional phenylene spacer, was treated with $Pd(BF_4)_2$ (DMSO-$d_6$, one hour, 50 °C) to give the expanded spherical complex **2c** in a quantitative yield. The structure of **2c** was confirmed by $^1$H NMR spectroscopy and CSI-MS. After diluting a DMSO solution of **2c** with $CDCl_3$, 500 equivalents of TMOS were added and the solution was stirred for four days at room temperature. Subsequent LDI-MS measurements confirmed the formation of silica nanoparticles with $M_n$ 31,570 Da and $M_w/M_n$ 1.004 (Fig. 3f). The TEM data showed a much larger silica nanoparticle with a diameter of 4.0 nm (Fig. 3d), which matched molecular modelling calculations (Fig. 4c).

Simply reducing the equivalents of TMOS generated smaller silica nanoparticles with surprisingly narrow distributions of molecular mass ($M_w/M_n$ <1.01). Addition of 130, 85 or 65 equivalents of TMOS to DMSO–$CHCl_3$ (1:9) solutions of **2a** resulted in silica nanoparticles with molecular masses and $M_w/M_n$ values (in parentheses) of 9,320 (1.008), 6,590 (1.009) and 5,200 (1.014), respectively (see Supplementary Information). However, when excess TMOS (340 equiv.) was added, silica gel and **2a** precipitated from the reaction mixture. After two days, no **2a** remained in solution, most likely a result of the insolubility caused by intermolecular cross-linking. The degree of silica condensation for the smaller nanoparticles could be estimated by $^{29}$Si magic-angle spinning (MAS) NMR measurements. Four broad peaks, $Q_1$, $Q_2$, $Q_3$ and $Q_4$, were observed ($Q_n$ was assigned to each possible $SiO_4$ product, that is $Si(OSi)_n(OH)_{4-n}$). As the molecular mass of silica nanoparticle increased, the $Q_n$ distribution reflected a higher degree of condensation (see Supplementary Information). The degree of condensation indicated that the density and surface area of the monodisperse silica nanoparticles can be controlled by tuning the equivalents of TMOS employed.

## Conclusions

We succeeded in the controlled synthesis of silica nanoparticles within the well-defined shell framework of self-assembled spherical hosts. Highly monodisperse silica nanoparticles (2–4 nm diameter), unobtainable by previous methods[10,11,27], were formed and fully characterized. We expect that this method will be applicable to the preparation of highly monodisperse nanoparticles of less than 10 nm of inorganic materials, such as various metal oxides, metal clusters and metal–organic frameworks, which could show new bulk properties and potential applications.

## Methods

**Self-assembly of 2a.** Ligand **1a** (105 mg, 0.200 mmol) was treated with a DMSO solution of $Pd(NO_3)_2$ (10 mM, 10.0 ml) at 50 °C for one hour. The quantitative formation of **2a** was confirmed by $^1$H NMR and CSI-MS. $^1$H NMR (500 MHz, DMSO-$d_6$): $\delta$ 9.24 (broad, 96H), 7.85 (broad, 96H), 7.68 (broad, 48H), 7.27 (broad, 24H), 4.97 (broad, 72H), 4.46 (broad, 72H), 4.32 (broad, 24H), 4.15 (broad, 24H), 3.93 (broad, 24H), 3.66 (broad, 24H), 3.25 (broad, 24H), 3.15 (broad, 48H), 3.02 (broad, 24H). Diffusion coefficient $D = 1.5 \times 10^{-10}$ m$^2$ s$^{-1}$ (DMSO-$d_6$:$CDCl_3$ = 1:9, 300 K). CSI-MS ($m/z$): calculated for $[\mathbf{2a}–12(NO_3^-)]^{12+}$, 1,173.7; found, 1,173.5.

**Self-assembly of 2c.** Ligand **1c** (65.5 mg, 0.100 mmol) was treated with a DMSO solution of $Pd(CH_3CN)_4(BF_4)_2$ (10 mM, 5.10 ml) at 50 °C for one hour. The quantitative formation of **2c** was confirmed by $^1$H NMR and CSI-MS. $^1$H NMR (500 MHz, DMSO-$d_6$): $\delta$ 9.31 (broad, 96H), 8.18 (broad, 96H), 7.96 (broad, 96H), 7.76 (broad, 96H), 7.61 (broad, 48H), 7.24 (broad, 24H), 4.95 (broad, 48H), 4.88 (broad, 24H), 4.51 (broad, 48H), 4.46 (broad, 24H), 4.30 (d, $J$ = 7.6 Hz, 24H), 4.25 (broad, 24H), 4.00 (broad, 24H), 3.66 (broad, 24H), 3.46 (broad, 24H), 3.18 (broad, 24H), 3.12 (broad, 48H), 3.05 (broad, 24H). Diffusion coefficient $D = 7.9 \times 10^{-11}$ m$^2$ s$^{-1}$ (DMSO-$d_6$:$CDCl_3$ = 1:3). CSI-MS ($m/z$): calculated for $[\mathbf{2c}–11(BF_4^-)]^{11+}$, 1,647.2; found, 1,647.5.

**Synthesis of silica nanoparticles within 2a. 2a** (14.6 μmol) in DMSO–$CHCl_3$–$H_2O$ (18.9, 166, 0.075 ml) was treated with TMOS (65, 85, 130, 170 equiv. for **2a**) at room temperature for four days. After all the TMOS had been hydrolysed, **2a**⊃silica was analysed by NMR, CSI-MS, LDI-MS, AFM and TEM. After the bulk of the solvent had been evaporated, ethyl acetate and diethyl ether were added to precipitate **2a**⊃silica. The solids obtained were washed with methanol and analysed by $^{29}$Si MAS NMR and XRF analysis.

- 65 equivalents of TMOS. Diffusion coefficient $D = 1.5 \times 10^{-10}$ m$^2$ s$^{-1}$ (DMSO-$d_6$:$CDCl_3$ = 1:9). CSI-MS ($m/z$, M = **2a** + silica (5,100 Da)):

$[M–8(NO_3^-)]^{8+}$, 2,430; $[M–9(NO_3^-)]^{9+}$, 2,150; $[M–10(NO_3^-)]^{10+}$, 1,930; $[M–11(NO_3^-)]^{11+}$, 1,750; $[M–12(NO_3^-)]^{12+}$, 1,605. LDI-MS: $M_n = 5{,}200$, $M_w = 5{,}270$ ($M_w/M_n = 1.013$). XRF analysis: number of silica atoms per **2a** was 66 (Pd:Si = 1:5.5). $^{29}$Si MAS NMR (59.7 MHz, MAS rate = 3 kHz): $Q_1$:$Q_2$:$Q_3$:$Q_4$ = 12:28:39:21 (−82.4, −91.5, −100.4, −109.2 parts per million (ppm)).

- 85 equivalents of TMOS. Diffusion coefficient $D = 1.5 \times 10^{-10}$ m$^2$ s$^{-1}$ (DMSO-$d_6$:$CDCl_3$ = 1:9). CSI-MS ($m/z$, M = **2a** + silica (6,400 Da)): $[M–8(NO_3^-)]^{8+}$, 2,590; $[M–9(NO_3^-)]^{9+}$, 2,290; $[M–10(NO_3^-)]^{10+}$, 2,060; $[M–11(NO_3^-)]^{11+}$, 1,870; $[M–12(NO_3^-)]^{12+}$, 1,715. LDI-MS: $M_n = 6{,}590$, $M_w = 6{,}650$ ($M_w/M_n = 1.009$). XRF analysis: number of silica atoms per **2a** was 83 (Pd:Si = 1:6.9). $^{29}$Si MAS NMR (59.7 MHz, MAS rate = 3 kHz): $Q_1$:$Q_2$:$Q_3$:$Q_4$ = 8:29:41:22 (−81.7, −91.5, −101.0, −109.9 ppm).
- 130 equivalents of TMOS. Diffusion coefficient $D = 1.5 \times 10^{-10}$ m$^2$ s$^{-1}$ (DMSO-$d_6$:$CDCl_3$ = 1:9). CSI-MS ($m/z$, M = **2a** + silica (9,000 Da)): $[M–9(NO_3^-)]^{9+}$, 2,585; $[M–10(NO_3^-)]^{10+}$, 2,320; $[M–11(NO_3^-)]^{11+}$, 2,100; $[M–12(NO_3^-)]^{12+}$, 1,920; $[M–13(NO_3^-)]^{13+}$, 1,770. LDI-MS: $M_n = 9{,}320$, $M_w = 9{,}390$ ($M_w/M_n$ = 1.008). XRF analysis: number of silica atoms per **2a** was 124 (Pd:Si = 1:10.3). $^{29}$Si MAS NMR (59.7 MHz, MAS rate = 3 kHz): $Q_1$:$Q_2$:$Q_3$:$Q_4$ = 6:27:42:24 (−82.4, −91.2, −100.7, −109.9 ppm).
- 170 equivalents of TMOS. Diffusion coefficient $D = 1.4 \times 10^{-10}$ m$^2$ s$^{-1}$ (DMSO-$d_6$:$CDCl_3$ = 1:9). CSI-MS ($m/z$, M = **2a** + silica (11,200 Da)): $[M–8(NO_3^-)]^{8+}$, 3,250; $[M–9(NO_3^-)]^{9+}$, 2,830; $[M–10(NO_3^-)]^{10+}$, 2,540; $[M–11(NO_3^-)]^{11+}$, 2,280; $[M–12(NO_3^-)]^{12+}$, 2,110. LDI-MS: $M_n = 11{,}020$, $M_w = 11{,}100$ ($M_w/M_n = 1.007$). XRF analysis: number of silica atoms per **2a** was 166 (Pd:Si = 1:13.8). $^{29}$Si MAS NMR (59.7 MHz, MAS rate = 3 kHz): $Q_2$:$Q_3$:$Q_4$ = 18:43:39 (−91.0, −100.5, −109.9 ppm).

**Synthesis of silica nanoparticles within 2c.** **2c** (4.17 μmol) in DMSO–$CHCl_3$–$H_2O$ (12.0, 35.7, 0.067 ml) was treated with TMOS (2.09 mmol, 500 equiv. for **2c**) and concentrated nitric acid (0.1 μl) at room temperature for four days. **2c**⊃silica was isolated and analysed in the same way as for **2a**⊃silica. Diffusion coefficient $D = 8.1 \times 10^{-11}$ m$^2$ s$^{-1}$ (DMSO-$d_6$:$CDCl_3$ = 1:3). LDI-MS: $M_n = 31{,}570$, $M_w = 31{,}690$ ($M_w/M_n = 1.004$). $^{29}$Si MAS NMR (59.7 MHz, MAS rate = 3 kHz): $Q_2$:$Q_3$:$Q_4$ = 7:50:43 (−91.2, −100.4, −109.2 ppm).

Full experimental details and crystallographic analysis (CCDC reference number 742085) are given in the Supplementary Information.

Received 14 August 2009; accepted 15 October 2009; published online 22 November 2009

## References


1. Alivisatos, A. P. Semiconductor clusters, nanocrystals, and quantum dots. *Science* **271,** 933–937 (1996).
2. Schmid, G. *Nanoparticles: from Theory to Application* (Wiley-VCH, 2004).
3. White, R. J., Luque, R., Budarin, V. L., Clark, J. H. & Macquarrie, D. J. Supported metal nanoparticles on porous materials. Methods and applications. *Chem. Soc. Rev.* **38,** 481–494 (2009).
4. Joo, S. H. *et al.* Ordered nanoporous arrays of carbon supporting high dispersions of platinum nanoparticles. *Nature* **412,** 169–172 (2001).
5. Fröba, M., Köhn, R., Bouffaud, G., Richard, O. & van Tendeloo, G. $Fe_2O_3$ nanoparticles within mesoporous MCM-48 silica: *in situ* formation and characterization. *Chem. Mater.* **11,** 2858–2865 (1999).
6. Yang, B., Kamiya, S., Yoshida, K. & Shimizu, T. Confined organization of Au nanocrystals in glycolipid nanotube hollow cylinders. *Chem. Commun.* 500–501 (2004).
7. Hermes, S. *et al.* Metal@MOF: loading of highly porous coordination polymers host lattices by metal organic chemical vapor deposition. *Angew. Chem. Int. Ed.* **44,** 6237–6241 (2005).
8. Pileni, M. P. Reverse micelles as microreactors. *J. Phys. Chem.* **97,** 6961–6973 (1993).
9. Kortan, A. R. *et al.* Nucleation and growth of CdSe on ZnS quantum crystallite seeds, and vice versa, in inverse micelle media. *J. Am. Chem. Soc.* **112,** 1327–1332 (1990).
10. Osseo-Asare, K. & Arriagada, F. J. Preparation of $SiO_2$ nanoparticles in a non-ionic reverse micellar system. *Colloids Surf.* **50,** 321–339 (1990).
11. Esquena, J., Tadros, Th. F., Kostarelos, K. & Solans, C. Preparation of narrow size distribution silica particles using microemulsions. *Langmuir* **13,** 6400–6406 (1997).
12. Dickerson, M. B., Sandhage, K. H. & Naik, R. R. Protein- and peptide-directed syntheses of inorganic materials. *Chem. Rev.* **108,** 4935–4978 (2008).
13. Vriezema, D. M. *et al.* Self-assembled nanoreactors. *Chem. Rev.* **105,** 1445–1489 (2005).
14. Douglas, T. & Young, M. Host–guest encapsulation of materials by assembled virus protein cages. *Nature* **393,** 152–155 (1998).
15. Douglas, T. *et al.* Protein engineering of a viral cage for constrained nanomaterials synthesis. *Adv. Mater.* **14,** 415–418 (2002).
16. McMillan, R. A. *et al.* Ordered nanoparticle arrays formed on engineered chaperonin protein templates. *Nature Mater.* **1,** 247–252 (2002).
17. Chasteen, N. D. & Harrison, P. M. Mineralization in ferritin: an efficient means of iron storage. *J. Struct. Biol.* **126,** 182–194 (1999).
18. Meldrum, F. C., Wade, V. J., Nimmo, D. L., Heywood, B. R. & Mann, S. Synthesis of inorganic nanophase materials in supramolecular protein cages. *Nature* **349,** 684–687 (1991).
19. Ueno, T. *et al.* Size-selective olefin hydrogenation by a Pd nanocluster provided in an apo-ferritin cage. *Angew. Chem. Int. Ed.* **43,** 2527–2530 (2004).
20. Tominaga, M. *et al.* Finite, spherical coordination networks that self-organize from 36 small components. *Angew. Chem. Int. Ed.* **43,** 5621–5625 (2004).
21. Kamiya, N., Tominaga, M., Sato, S. & Fujita, M. Saccharide-coated $M_{12}L_{24}$ molecular spheres that form aggregates by multi-interaction with proteins. *J. Am. Chem. Soc.* **129,** 3816–3817 (2007).
22. Tominaga, M., Suzuki, K., Murase, T. & Fujita, M. 24-Fold endohedral functionalization of a self-assembled $M_{12}L_{24}$ coordination nanoball. *J. Am. Chem. Soc.* **127,** 11950–11951 (2005).
23. Sato, S. *et al.* Fluorous nanodroplets structurally confined in an organopalladium sphere. *Science* **313,** 1273–1276 (2006).
24. Suzuki, K., Kawano, M., Sato, S. & Fujita, M. Endohedral peptide lining of a self-assembled molecular sphere to generate chirality-confined hollows. *J. Am. Chem. Soc.* **129,** 10652–10653 (2007).
25. Van Bommel, K. J. C., Friggeri, A. & Shinkai, S. Organic templates for the generation of inorganic materials. *Angew. Chem. Int. Ed.* **42,** 980–999 (2003).
26. Yamaguchi, K. Cold-spray ionization mass spectrometry: principle and applications. *J. Mass Spectrom.* **38,** 473–490 (2003).
27. Stöber, W., Fink, A. & Bohn, E. Controlled growth of monodisperse silica spheres in the micron size range. *J. Colloid Interface Sci.* **26,** 62–66 (1968).


## Acknowledgements

We thank M. Kawano for supporting the synchrotron X-ray crystallographic analysis at Photon Factory-Advanced Ring for Pulse X-rays of the High Energy Accelerator Research Organization. This work was supported by the Core Research for Evolution Science and Technology project of the Japan Science and Technology Agency, for which M.F. is the principal investigator, and also in part by the Global COE Program (Chemistry Innovation through Cooperation of Science and Engineering), Ministry of Education, Culture, Sports, Science and Technology (MEXT), Japan. A part of this work was conducted in the Center for Nano Lithography & Analysis, The University of Tokyo, supported by MEXT, Japan. This work was approved by the Photon Factory Program Advisory Committee.

## Author contributions

M.F. designed and directed the project and wrote the manuscript. K.S. performed the experimental work and wrote the manuscript. S.S. contributed to the data analysis.

## Additional information

The authors declare no competing financial interests. Supplementary information and chemical compound information accompany this paper at www.nature.com/naturechemistry. Reprints and permission information is available online at http://npg.nature.com/reprintsandpermissions/. Correspondence and requests for materials should be addressed to M.F.